NGU Report 2000.070

Fracture lineaments, Cenozoic(?) faults, and Mesozoic extenisional tectonics of the Møre Trøndelag region, central Norway

NGU
Norges geologiske undersøkelse
Geological Survey of Norway
Geological Survey of Norway
N-7441 Trondheim, Norway
Tel.: 47 73 90 40 00
Telefax 47 73 92 16 20

REPORT

Report no.: 2000.070 | ISSN 0800-3416 | Grading: Open

Title:
Fracture lineaments, Cenozoic(?) faults, and Mesozoic extenisional tectonics of the Møre Trøndelag region, central Norway.

Authors:
T. F. Redfield, R. H. Gabrielsen, and T. H. Torsvik

Client:
VISTA

County:
Nord-Trøndelag and Sør-Trøndelag

Commune:

Map-sheet name (M=1:250.000)

Map-sheet no. and -name (M=1:50.000)

Deposit name and grid-reference:

Number of pages: 33 Price (NOK): Kr. 145,-

Map enclosures:

Fieldwork carried out: April-August 1999

Date of report: Mai 2000

Project no.: 281500

Person responsible: Jan S. Rønning

Summary:
A map of all lineaments resolvable at 1:100,000 scale on a LandSAT TM5 image utilizing bands 1, 2, and 3 was constructed over the Møre Trøndelag region of central Norway. This onshore fracture lineament map was merged with an offshore lineament map constructed from 500 meter grid bathymetric data and with maps of potential field data. Analysis of the fracture lineament map resolved a high density region in the north of the study area and a low density region to the south. NW-SE trending fracture lineaments show the greatest variation in density, followed by NE-SW trending lineaments. Densities of N-S and E-W trending lineaments are unaffected by geography.

By combining lineament patterns with lineament density grids, topographic and bathymetric data, marine and onshore magnetic and gravity data, field data, and published apatite fission track (AFT) ages we identified three geotectonic blocks. AFT ages within each block are concordant at the 95% confidence level. The AFT ages of the blocks increase from SE to NW and are statistically discrete. Cross sections show that the blocks define a step function topography descending to the NW. Although not precluding strike slip, the data suggest vertical tectonics were important during the Mesozoic and Cenozoic development of the MTFC.

Field studies on Vikna Island and the Fosen Peninsula have shown that several lineaments in mid Norway are faults of more than local importance. Steep dip-slip slickenlines on two NE trending fault planes are accompanied by wide damage zones, and a NS trending fault exhibits low angle (strike slip) slickenlines, extensive brecciation, and cataclasis. On the lineament map, these faults appear as short (<5km) structures forming rhombic intersections with strongly expressed NE-SW lineaments. We interpret these faults to bound small-scale duplex structures within a larger extensional or transtensional system that exhumed and juxtaposed the three geotectonic blocks.

The AFT data and regional geological considerations suggest final juxtaposition and exhumation of the blocks took place during Cretaceous or Tertiary (possibly Neogene) time. We suggest that at least some of the fracture lineaments of central Norway were re-activated during Mesozoic extension and the opening of the Norwegian sea.

Keywords: Berggrunn	Geofysikk	Fjernanalyse
Forkastning	Fagrapport	

CONTENTS

1. INTRODUCTION

Early satellite image studies over central Norway defined large-scale geological structures such as the Møre Trøndelag Fault Complex (MTFC) and other extensive systems of faults, fractures, and lineaments (e.g. Gabrielsen and Ramberg, 1979; Ramberg et al., 1977; Rindstad and Grønlie, 1986). The fracture patterns first reported by Kjerulf (1879) and Hobbs (1911) are widespread, prominent elements of Norwegian bedrock geology. Since then, image analysis and Geographic Information Systems (GIS) programs have made possible new methods of analysis of lineament patterns, and facilitated the integration of results with regional and local geologic data.

Although the almost complete dearth of onshore post-Paleozoic sedimentary rocks led previous workers to suggest significant Tertiary exhumation of Scandinavia (e.g. Holtedahl, 1953; Torske, 1972), limitations imposed by the tools of the day precluded recognition of corresponding post-Permian onshore faulting. However, modern petrologic and chronological studies have uncovered evidence of widespread faulting. Local extensional activity beginning shortly after the peak of Caledonian compression (e.g. Fossen and Dunlap, 1988) became continental in scale during the Mesozoic. Episodes of late Paleozoic, Mesozoic and possibly early Cenozoic reactivation have been suggested for the Verran fault of the MTFC (Torsvik et al., 1989; Grønlie et al., 1994; Grønlie and Roberts, 1990), the Dalsfjord Fault (DF; Torsvik et al., 1992), the Lærdal-Gjende Fault System (LGFS; Milnes and Koestler, 1985; Andersen et al., 1999), and the Hjeltefjord Fault (Fossen et al., 1997). Offshore, geophysical studies and borehole sampling have shown that graben development and faulting continued until the Cretaceous or early Tertiary (e.g. Doré et al., 1999). The unequivocal record of Mesozoic extension in the North and Norwegian Seas and the growing evidence of Mesozoic faulting onshore suggests that at least some of the fracture lineaments formed or were reactivated as tectonic structures at that time.

In this account we mapped lineaments using three LandSAT 5 TM scenes covering the MTFC and surrounding areas in Norway and western Sweden (Figure 1). We then merged the lineament maps with onshore and offshore geophysical data. Lastly, using geomorphic, geologic, and geochronologic data we formulated a testable model consistent with the known Mesozoic geotectonic history of central Norway and the extensional history of the Norwegian Sea.

2. POST CALEDONIAN FAULTING

A simplified geological map of southern Norway shows autochthonous and parautochthonous Baltic shield basement covered by three Caledonian allochthons: Baltic cover, Baltic basement and cover, and rocks of ophiolitic and island arc affinity (Figure 1; e.g. Bryhni and

Sturt, 1985; Gee et al., 1985). Two major structural zones, the MTFC and the Hardangerfjord Shear Zone (HSZ), slash southwest across the map and rampage out to sea.

The MTFC is comprised by two principal fault strands, the Hitra-Snåsa fault and the Verran fault. Previous workers have proposed an extensive and sometimes contradictory Paleozoic and early Mesozoic history for the MTFC (Roberts, 1983; Buckovics et al., 1984; Fossen, 1998; Bøe and Bjerklie, 1989; Grønlie and Roberts, 1989; Torsvik et al., 1989; Seranne, 1992). Most recently, Gabrielsen et al. (1999) postulated early Devonian sinistral transpression followed by late Permo-Triassic dextral transtension, possibly extending into the Jurassic and early Cretaceous.

Several studies have specifically addressed the timing of faulting along structures comprising the MTFC. Grønlie and Roberts (1989) interpreted dextral strike slip duplexes between the Verran and Hitra-Snåsa faults to be of Mesozoic age. Supporting their conclusion, fault related Mesozoic paleomagnetic overprints have been resolved in several locations along the MTFC (Torsvik et al., 1989; Grønlie and Torsvik, 1989). Weighing in from the geochronological perspective, Grønlie et al (1994) reported a late Jurassic cooling event along the Verran fault of the MTFC, recorded by apatite, zircon, and sphene fission track data. Grønlie et al. (1994) measured fission tracks in flourite (an experimental technique) and suggested late Cretaceous or Cenozoic fault activity may also have occurred.

The HSZ forms a tectonic zone subparallel to both the MTFC and the Permo-Carboniferous volcanics of the Oslo Rift (Figure 1). Seismic reflection data show that the HSZ is a major structural discontinuity projecting offshore as far as the Horda Platform (e.g. Hurich and Kristofferson, 1988). A stratigraphically controlled seismic section interpreted by Ditcha (1998) shows widespread Permo-Triassic, Jurassic, and some Cretaceous to Tertiary displacement across faults splaying from the offshore continuation of the HSZ (see also Hurich and Kristofferson, 1988). Onshore, the HSZ was responsible for excision of tectonostratigraphy and exhumation of Fennoscandian basement, and may form a continuous structure with the Lærdal-Gjende Fault System (LGFS; Andersen et al., 1999). Paleomagnetic data show some of the brittle, down to the west normal faults of the LGFS may have been active circa mid-late Permian and late Jurassic (Andersen et al., 1999).

The Nordfjord Sogn Detachment (NSD; Figure 1) forms the boundary between Precambrian crystalline basement and tectonostratigraphically overlying Caledonian and Devonian units. Using paleomagnetism, Torsvik et al. (1992) concluded the low-angle Dalsfjord Fault (part of the Nordfjord Sogn detachment; Figure 1) underwent Permian and Upper Jurassic or Lower Cretaceous reactivation. Using 40Ar/39Ar technique Eide et al. (1997) resolved Permo-Triassic and Late Jurassic Early Cretaceous overprint ages for the same rocks, supporting the conclusions of paleomagnetic fault dating studies in southern and central Norway.

These data strongly indicate that significant onshore faulting occurred during the Mesozoic and possibly the Cenozoic throughout southern Norway. This period of onshore tectonism is

contemporaneous with major extensional movements on the offshore continental shelf, and was probably extensional in nature as well.

3. LINEAMENT MAPS

The fracture lineament patterns of western Norway mark zones of weakness that may have existed since Paleozoic or even Precambrian times (Gabrielsen and Ramberg, 1979; Coward, 1990 Doré et al., 1999, Færseth et al., 1995; Gabrielsen et al, 1999). Some fracture lineaments are known to be faults, several of which may have been reactivated in the Mesozoic (see above) or even post glacial times (e.g. Olesen, 1988).

Detailed field studies of individual lineaments and faults hidden within them remain critical to understanding the post-Paleozoic structural development of onshore central Norway. However, remote sensing and GIS can help create a regional framework within which to interpret the relative importance of each newly identified fault. To that end we conducted a *haute technologie* survey of the lineaments of the Møre Trøndelag area.

Three LandSAT scenes were georectified using 1:250,000 vector files delimiting the Norwegian coastline, rivers, and large bodies of water, and a simple red green blue mosaic image constructed from bands 1, 2, and 3. Lineaments were mapped on the computer image as complex digital polylines within a GIS framework, accurately maintaining XY geographic information. The map entirely covers the MTFC and nearby areas (Figure 2a).

Marine bathymetric lineaments resolvable on a 500 meter grid digital elevation model were mapped to provide offshore continuity. Bathymetric lineaments were selected qualitatively from a pseudocolor image using 2D and 3D views with a range of synthetic sun shade angles and horizontal and vertical scales. However, the bathymetric coverage is poor to non-existant near the coast and in the fjords. We did not include the bathymetric lineaments in our quantitative analysis of onshore fracture lineament directions and densities.

The mapped lineaments obey a power law distribution with a misfit at either end of the length spectra (Figure 2b). The best power law fit is obtained for lineaments between ~3km and ~24km in length. The power law misfit of longer lineaments may be explained by incomplete sampling: longer lineaments run off the edge of the images and their populations are not fully represented. Also, tectonic factors such as horizontally changing stress fields might impose a fundamental upper limit to the length of a lineament. The misfit of lineaments shorter than 3km is probably due to a combination of factors, such as variations in bedrock exposure or the limits of LandSAT 5 TM resolution

The significance of power laws with respect to scale independent phenomenon such as fractures is a subject of debate. However, the power law does provide a means of quality

discrimination. Marrett et al. (1999) showed the lengths of a well-constrained data set of natural faults and extension fractures to be consistent with a power law distribution across nearly five orders of magnitude, with no natural gaps or changes in size distributions. Accordingly, we focused our analysis on those data that best meet the power law distribution by filtering the lineament map to include only data between 3km and 24km in length (Figure 2c).

4. LINEAMENT DESCRIPTIONS

Figure 3 shows length-weighted lineament azimuth distributions of the filtered and unfiltered data. The principal difference between the two data sets are very small peaks at ~025 and ~090 in the filtered group. We interpreted the peaks to be significant and split the filtered data into five populations by azimuth: N-S (345 to 025), NE-SW (025 to 085), E-W (085 to 100 and 100 to 120), and NW-SE (120 to 165).

Many of the NE-SW lineaments are parallel to a pervasive and strongly expressed Caledonian foliation, and thus cannot be easily distinguished as post-Caledonian structures. However, some of the NE-SW lineaments clearly crosscut the foliation, indicating at least some of the population are younger than the Caledonian allochthons. Where possible, foliation was identified and discarded. Collectively the NE-SW lineaments form strongly expressed, continuous, deeply incised linear to curvilinear systems spaced some 10km to 20km apart. Particularly near the MTFC, individual lineaments can be discontinuous with branching or stepping map traces forming rhombs and frayed, dendritic patterns at their ends. In terms of length and continuity these lineaments dominate the study area.

The NW lineaments are continuous to discontinuous, linear to curvilinear, sometimes stepping segments that commonly branch into dendritic and frayed patterns near the coast. Many NW lineaments intersect the major NE lineament groups, including the Hitra-Snåsa and Verran faults. However, clear cross cutting relationships permitting relative age determination are not observed.

The NS lineaments are discontinuous, linear to curvilinear segments, occurring less commonly throughout the area. They exhibit few branching or stepping patterns, and their paucity gives an older, overprinted appearance on the lineament map. The NS population may have been part of a pre-existing post Caledonian or even Precambrian structural grain (e.g. Coward, 1990; Færseth et al., 1995).

The EW lineaments occur throughout the area as discontinuous, regularly but widely spaced individual structures. Two azimuth sub-populations occur but rarely intersect. The EW lineaments also appear overprinted by the NE and NW structures, and may also be an expression of an older fabric.

5. LINEAMENT DENSITY DISTRIBUTION

Lineament densities were computed for populations of all lineaments and lineaments segregated by length and azimuth. Densities were computed for both raw lineament data and for lineament data weighted by length. Grid cell sizes were 10km, 5km, and 2.5km. Some examples are shown in Figure 4. Common to all grids is a pronounced density contrast across a wide zone coincident with the general area of the MTFC. The highest lineament densities are found on the Fosen Peninsula, north and outboard of the MTFC.

Photographically mapped areas of high fracture density might be expected to correlate with areas of better bedrock exposure on lightly vegetated areas such as the Fosen Peninsula. However, a LandSAT map of well exposed (lightly vegetated) regions and poorly exposed (heavily vegetated) regions exhibits very little correlation with the zones of high and low fracture density (Figure 5a). Alternatively, differences in lithology might play an important role in determining fracture lineament density. In general, the low density area south of the MTFC correlates positively with the simplified contacts of the homogeneous Western Gneiss Region (WGR). However, a length weighted density plot of the NW-SE family of lineaments shows strong variations within the WGR, indicating rheology is not the only controlling factor (Figure 5b).

6. POST CALEDONIAN FAULTING, PART TWO

During the past thirty years the importance of brittle deformation processes has been increasingly recognized. While the lineaments of western Norway were traditionally regarded as geomorphic features of minor tectonic significance, recent studies have upgraded a steadily increasing number of lineaments into full fledged faults (e.g. Fossen, 1998).

During 1999 we engaged in field studies of several lineaments on the Fosen Peninsula and Vikna Island (Figure 1). At least two lineaments on Vikna are known to be faults of regional importance. One NNE trending fault *neè* lineament, exposed in a roadside outcrop 1km east of Drag village, incorporates at least three lenses of lithologically distinct fault breccias separated by surfaces carrying steep slickensides (Figure 6a). Net vertical offset must have been of sufficient magnitude to incorporate fragments of mylonite in coarse, brittlely deformed breccias. In nearby Grindvikna village another NNE fault exposes multiple lenses of lithologically distinct breccias, steeply dipping slickenlines carried on epidotized surfaces, calcite/epidote/sulfide mineralization, and an unconsolidated fault gouge (Figure 6a). Near Osen village on the Fosen Peninsula, several NW trending lineaments expose damage zones exhibiting various deformation products including breccia, cataclasite, mylonite(?), and possibly pseudotachylite (Olsen, pers. comm.; Olsen et al., 1999). Also near Osen, a

spectacular damage zone containing coarse breccias, calcite/sulfide mineralization, cataclasite lenses, and unconsolidated fault gouge is well exposed in a N-S trending lineament (Figure 6a). Low angle slickenlines clearly demonstrate that the most recent movements across this fault were strike slip.

Although the Drag, Grindvikna, and Osen faults are individually spectacular structures, they appear on the LandSAT TM5 image as relatively short lineaments. However, the regional lineament geometry suggests a relationship exists between the faults and the more strongly expressed NE lineaments (Figure 6b). The NNE trending Drag and Grindvikna faults are subparallel to one another, their projected traces are left stepping, and they form rhomboid intersections with NE-SW trending lineaments that are parallel to the MTFC. The Osen Fault is one of a number of short, N trending lineaments near a major complex of NE-SW structures. The fault forms a very low angle intersection with a NW trending lineament exposing a less extensively brecciated damage zone. Other nearby NW trending lineaments also expose deformation products. Extensive, deeply incised NE-SW lineaments parallel to the MTFC and the regional Caledonian nappe foliation sandwich the smaller structures (Figure 6b).

A general rhombic, low angle relationship exists between the proven faults, potential faults, and the NESW trending lineaments, raising the possibility that the smaller structures are bounding duplexes, helping transfer strain between much larger, much more important faults (see also Grønlie and Roberts, 1989).

7. TECTONIC INTERLUDE

From LandSAT mapping we concluded that NW-SE and NE-SW lineaments occur in a northern high density zone and a southern zone of relatively low density. From our field studies we concluded that some of the lineaments are faults, and are likely to be smaller structures within regionally important fault systems. We next combined literature data published by earlier workers with our lineament map and field data to create a testable post-Paleozoic regional tectonic model for the MTFC and its adjacent areas.

Strong magnetic lineaments parallel the Hitra Snåsa strand of the MTFC and continue offshore (Olesen et al., 1997; Figure 7). Enhanced gravity data reveal a similar pattern (Fichler et al., 1999). The geophysical data correlate with the onshore trace of the Hitra-Snåsa strand of the MTFC (Figure 7). Where data are availible, bathymetric lineaments compare well with the onshore/offshore geophysical lineaments. Strongly expressed NE trending lineaments south of the MTFC also correlate with onshore/offshore magnetic lineaments, bathymetric lineaments, and the enhanced gravity map. Further inland, the geophysical and lineament trends become more diffuse, but can still be interpreted as a wide structural zone.

Topographic/bathymetric cross sections were drawn across the study area (Figure 8a). On each section we located the Hitra-Snåsa fault and the more diffuse structural zone to the south defined by geophysical anomalies and lineament densities. We then calculated the cross sectional area beneath the topographic profiles (e.g. the Rieman sum) to determine the cross sectional area of the inner, middle, and outer zones. From area and width we calculated the average elevation. A step function topography descending to the NW is evident (Figure 8b). We suggest the three zones represent discrete structural blocks of regional scale, tectonically separated from one another by regional fault systems with strong components of vertical offset.

By dividing each length-weighted azimuth histogram category by the area of its tectonic block we created normalized azimuth distribution diagrams, permitting quantitative comparison of peaks and valleys between the three blocks. Although the azimuth trends do not change significantly from one block to the next, the density of lineaments does (Figure 8c). Fracture densities of the NE-SW and NW-SE lineaments decrease from NW to SE while the fracture densities of the NS and EW lineaments are unaffected by geography. The NW-SE structures are the most geographically dependant, exhibiting more than twice the normalized density in the outer block than from the middle or inner blocks (Figure 8c). Gabrielsen et al. (1999) and Pascal and Gabrielsen (in press) speculated that the MTFC may have acted as a buffer between a northerly stress regime favoring formation or reactivation of NW lineaments and a southerly stress regime less favorable to NW structural trends; our data support their conclusion.

8. THERMOCHRONOMETRY

In the absence of stratigraphic markers, low temperature age data can provide critical structural information. We next examined existing age data from the area to place some thermochronometric constraints upon our tectonic interpretation.

Eleven AFT ages published by Grønlie et al. (1994), Rohrman (199?), and Rohrman et al. (1995) lie within our study area. Also, Stiberg (1993) and Stiberg and Mørk (1998) presented four preliminary ages. We list these ages and supplementary information in Table 1. Statistics describing each AFT age are found in the original publications.

There are many pitfalls into which one can blunder whilst interpreting fission track ages, especially literature ages published by other workers. Nevertheless, AFT data are a powerful tool with which to identify different structural blocks and compare their histories of exhumation. Gallagher et al. (1998) provided a thorough review of the fission track method and its application to geological problems. Referring the reader to their article for details, we note several considerations that are important to our use of the existing AFT data.

Because the rate of annealing of fission tracks in apatite is a function of both time and temperature, an AFT age does *not* represent the passage of the sample below a single critical isotherm. For example, when extrapolated to geological time scales the laboratory experiments of Laslett et al. (1987) suggested annealing occurs between 60°C and 110°C with a 10°C uncertainty. Therefore, relating a fission track age to a closure temperature is only plausible when it can be demonstrated that no significant annealing has occurred post-closure time (Gallagher et al., 1998). Although not all of the ages quoted in our study were published with track length data, the available length histograms and modeled ages indicate that cooling to below 60°C was slow rather than rapid. Thus, a fixed closure temperature is not valid for the AFT ages within our study area.

Many workers have demonstrated the sensitivity of AFT ages to changes in elevation, particularly where rapid exhumation enabled the preservation of a fossil PAZ (e.g. Fitzgerald and Gleadow, 1988). Rapidly cooled samples of statistically different ages from common elevations could be expected to unambiguously resolve structural offset. However, slow cooling within a PAZ, exposure to a lateral thermal gradient, or both, could cause widely separated rocks of similar elevation within a homogeneous structural block to record very different AFT ages. By stacking four vertical profiles and shifting their base elevations by as much as 2000 meters Rohrman et al. (1995) interpreted the Hunnedalen sample suite of Andriessen (1990) to be an exhumed Jurassic PAZ. There, within a zone of ~300 vertical meters AFT ages span ~160Ma to ~240Ma. If their interpretation is correct, AFT ages of common elevations from a Jurassic PAZ in western Norway might be expected to range widely, perhaps by as much as ~80Ma.

With these caveats firmly in mind we proceeded to examine the previously published AFT data from our study area.

Four finalized AFT ages published by Rohrman (1995) and Rohrman et al. (1995) lie within the inner block and are concordant between 124Ma and 128Ma at the 95% confidence level (Figures 9a, 9b). One of the samples yielded enough confined tracks for a good length measurement. The length data (12.5 +/- 0.2 microns, standard deviation 1.5; no published histogram) suggested slow cooling.

Grønlie et al. (1994) published AFT ages from in and around the MTFC. Their study focused on the age of the MTFC itself, rendering several samples unsuitable for assessing exhumation of the country rock. However, considerable exhumation information can be gleaned from their study.

Six samples from Grønlie et al (1994) lie within the middle block. Of these, sample AG1 was collected from a strongly hydrothermally altered zone with abundant stilbite and laumontite mineralization within the Verran fault (Grønlie et al., 1994). We discarded it as not representative of the cooling history of the country rock. Two other samples (FT2 and FT5) were also collected from hydrothermally altered zones. However, their AFT ages and the

ages of the remaining two samples (AG2 and AG3) are concordant at the 95% confidence level between 203Ma and 224 Ma (Figures 9a, 9b), suggesting Triassic or Jurassic AFT exhumation of these rocks.

The exhumation of the outer block is less constrained. Grønlie et al. (1994) reported an AFT age of 167Ma +/-20 for sample AG4, located near Åfjord (Figure 9b). However, this age is incompatible with a preliminary AFT age of 315Ma near Roan reported by Stiberg (1993). Neither sample appears reset: the histogram of AG4 (13.95 +/-0.13 microns, standard deviation 1.30) shows no indication of bimodal distribution, and Stiberg (1993) described track length measurements from the Roan sample as typical of undisturbed basement.

We have no reason to discard sample AG4. However, we note its location is very close to a major lineament system parallel to the MTFC and whose offshore extension can clearly be seen in the bathymetric data (Figure 9b). We speculate AG4 was inadvertantly collected from a minor fault block that is tectonically seperated from Stiberg's 315Ma Roan sample. Additional preliminary AFT ages from the Froan Archipelago and the Fosen Peninsula (northwest of the MTFC) are in the order of 260Ma to 320Ma (Stiberg and Mørk (1998), supporting our interpretation.

Because the Roan sample is not adjacent to a major lineament system, we interpret it to be representative of the exhumation of the outer block. Because the 91 m.y. difference between the 315Ma Roan age and the 224Ma upper limit of concordance of the middle block ages is greater than the ~80 m.y. span of the possible exhumed Jurassic PAZ of the Hunnedalen suite of Andriessen (1990), we suggest the ages of exhumation of the outer and middle blocks are statistically discrete. The oldest, highest AFT ages of the Jotunheim vertical profile of Rohrman et al. (1995) represent the maximum plausible AFT ages for the inner block. Because the highest Jotumheim ages do not overlap the 203Ma lower limit of concordance of the middle block ages (Figure 9a), we interpret the inner and middle blocks to have been exhumed at statistically discrete times.

9. DISCUSSION

Although it is not possible to assign an absolute closure temperature to the AFT data, it is known the ages were "set" somewhere between ~60°C and ~110°C (e.g. Gallagher et al., 1998). Assuming a paleogeothermal gradient of 25°C /km and a mean Paleo- Average Annual Surface Temperature (PAAST!) of 10°C the AFT ages reflect cooling within a zone some 2 km to 4 km deep. In turn, this suggests a minimum of 2km overburden was removed from each block since the time of cooling. The ~200 million year cooling difference between the inner and outer blocks indicates they were subjected to very different exhumation pathways.

Figure 10 shows a schematic model depicting regional rock column exhumation accompanied by down-to-the-NW relative movement between blocks. The model is related to a lithospheric scale cross section by Mosar (2000) drawn from a land to sea deep seismic section interpreted by Hurich and Roberts (1997) and from regional geology. The three blocks defined by our analysis may have formed as Caledonian thrusts and been reactivated with dip slip components.

Minor deposits of Jurassic age sedimentary rocks west of Kristiansund have been interpreted to indicate that the underlying basement has been at or near sea level since that time (e.g. Stiberg and Mørk, 1998). These rocks are adjacent to the MTFC and are likely tectonic slivers of the outer block, which has undergone the least amount of exhumation (Figure 10).

Our model does not preclude the major strike slip activity postulated for the MTFC by Serranne (1992), Gabrielsen et al. (1999), or others. However, from the available thermochronometric data we conclude that any strike slip model must incorporate a major net vertical component of relative motion across the MTFC. The circa 125Ma sea level AFT ages recorded within the inner block suggest that a large net vertical offset occurred during Cretaceous or even early Tertiary times. This is compatible with age and track length modeling of AFT data by Rohrman (1995) and Rohrman et al. (1995), who concluded southern Norway was affected by a first phase of Mesozoic/Cenozoic exhumation related to offshore extension and a second phase that began in the Neogene circa 30Ma. It is also compatible with offshore geological data: in a review of tectonic and stratigraphic data from the Vøring Basin, Lundin and Doré (1997) suggested an extensional tectonic event of mid Cretaceous age occurred in the Norwegian Sea. Final exhumation of the blocks (accompanied by down to the northwest relative motion between blocks) may have occurred as late as ~30Ma, possibly a result of changes in North Atlantic relative plate motions at that time Torsvik et al. (2000).

Although it is propably not likely that any single lineament mapped during this project is a fault of lithospheric scale, we consider it very probable that the fracture systems characterized by high lineament densities and geophysical anomalies marking the block boundaries constitute pervasive, structurally interconnected zones of weakness that extend to great depths. Within these zones, older faults could be reactivated and new faults formed in response to changes in orientation and intensity of ridge push induced stress.

10. CONCLUSIONS

LandSAT TM5 image analysis shows the northern part of the Møre Trøndelag region of western Norway is characterized by higher lineament densities the southern part. The NW trending structures make the most important contribution to the high density area. The MTFC may have acted as a buffer between a northerly stress regime favoring formation or

reactivation of NW lineaments and a southerly stress regime less favorable to NW reactivation.

Field studies have shown some of the fracture lineaments are relatively large faults. We suggest these faults helped transfer strain generated along regional fault systems that trend dominantly NE, parallel and sub parallel to the main trend of the MTFC. From lineament data, potential field data, topographic data, published geological data, and published AFT data, we conclude that the Møre Trøndelag region is comprised by at least three fault bounded geotectonic blocks which must have significantly different cooling histories - in short, *terranes of exumation.*

Although the data do not preclude large components of strike slip offset across the MTFC, we interpret the AFT data to require a large net component of down to the west relative motion between the inner, middle, and outer blocks. The circa 125Ma AFT ages from sea level sites within inner block suggest the fault systems bounding the blocks were active during the Cretaceous or later. Time temperature path modeling of AFT data from southern Norway by Rohrman et al. (1995) suggested exhumation occurred in two phases: Mesozoic, and Neogene (circa 30Ma). Their modeled time temperature paths open the possibility that the inner block to middle block bounding structure was active circa 30Ma. In turn, this raises the possibility that many faults and yet-to-be-discovered faults hiding in the fracture lineaments of the Møre Trøndelag region were tectonically active during the Cenozoic.

11. ACKNOWLEDGEMENTS

Acknowledgements. - The authors are grateful to many people. John Dehls (NGU) provided invaluable assistance with the LandSAT imagery. David Roberts, Elizabeth Eide, and John Mosar (NGU) and Agust Gudmundsson and Wojtec Nemec (UiB) are thanked for critical reviews and hours of scintillating discussion and advice. Elin Olsen and Kelfrid Lyslo (UiB) helped with the field mapping. Kinematic Stress Strain (KiSS) is a VISTA sponsored project.

12. REFERENCES

Andersen, T. B., Jamtveit, B., Dewey, J. F., & Swensson, E. 1991: Subduction and education of continental crust; major mechanisms during continent-continent collision and orogenic extensional collapse. *Terra Nova* 3, 303-310.

Andersen, T. B., Torsvik, T. H., Eide, E., Osmundsen, P. T., & Faleide, J. 1999: Permian and Mesozoic extensional faulting within the Caledonides of central south Norway. *Journal of the Geological Society* London, vol. 155.

Andriessen, P. A. M. 1990: Anomalous fission track ages of the Precambrian basement in the Hunnedalen region, south-western Norway. *Nucl. Tracks Radiat. Meas.* 17, 285-291.

Bryhni, I. & Sturt, B. A. 1985: Caledonides of southwestern Norway. *In* Gee, D. & Sturt, B. A. (eds.): *The Caledonide Orogen - Scandinavia and Related areas,* 89-106. John Wiley & Sons, Chichester.

Buckovics, C., Cartier, E. G., Shaw, N. D. & Ziegler, P. A. 1984: Structure and development of the mid Norwegian continental margin. *In* Spencer (ed.), *Petroleum Geology of the North European Margin.* 407-423. Graham and Trotman, London.

Bøe, R. & Bjerklie, K. 1989: Mesozoic sedimentary rocks in Edøyfjorden and Beitstadfjorden, Central Norway: Implications for the structural history of the Møre Trøndelag Fault Zone. *Marine Geology.* 87, 287-299.

Coward, M. P. 1990: Structural and tectonic setting of the Permo-Triassic basins of northwest Europe. *In:* Boldy, S. A. R. (ed.), *Permian and Triassic rifting in northwest Europe,* Geological Society, London, Special Publications, 91, 7-39.

Ditcha, E. 1998: Pre-Tertiary evolution of the Stord Basin. *Cand, Scient. Thesis*, Univ. Oslo.

Doré, A. G., Lundin, E. R., Jensen, L. N., Birkeland, Ø, Ellesen, P. E., & Fichler, C. 1999: Principal tectonic events in the evolution of the northwest European Atlantic margin. *In:* Fleet, A. J. and Boldy, S. A. R. (eds.), *Petroleum Geology of Northwest Europe: Proceedings of the 5th Conference*. 41-61, Geological Society, London.

Eide, E. A., Torsvik, T. H. & Andersen, T. B., 1997: Absolute dating of fault breccias: Late Palaeozoic and early Cretaceous fault reactivation in Western Norway. *Terra Nova, 9,* 135-139.

Fichler, C., Rundhovde, E., Olesen, O., Sæther, B. M., Rueslåtten, H., Lundin, E., & Doré, A. G. 1997: Regional tectonic interpretation of image enhanced gravity and magnetic data covering the mid-Norwegian shelf and adjacent mainland, *Tectonophysics*, 306, 183-197.

Fitzgerald, P. G., & Gleadow, A. J. W. 1988: Fission track geochronology, tectonics, and structure of the Transantarctic Mountains in Northern Victoria Land, Antarctica. *Chem. Geol.* 73: 169 - 178.

Fossen, H. 1992: The role of extensional tectonics in the Caledonides of southern Norway. *Journal of Structural Geology* 14, 1033-1046.

Fossen, H. 1992: Indication of transpressional tectonics in the Gullfaksoil field, northern North sea. *Marine and Petroleum Geology.* 6, 22-30.

Fossen, H., 1998: Advances in understanding the post-Caledonian structural evolution of the Bergen Area, West Norway, *Norsk Geologisk Tidskrift*, 78, 33-46.

Fossen, H. & Dunlap, W. J. 1986: Timing and kinematics of Caledonian thrusting and extensional collapse, southern Norway: evidence from 40Ar/39Ar thermochronology, *Journal of Structural Geology*, 20, 6, 765-781.

Fossen, H., Mangerud, G., Hesthammer, J., Bugge, T., & Gabrielsen, R. 1997: The Bjorøy Formation: a newly discovered occurance of Jurassic sediments in the Bergen Arc system, *Norsk Geologisk Tidskrift*, 77, 269-287.

Færseth, R. B., Gabrielsen. R. H., & Hurich, C. A. 1995: Influence of basement in structuring of the North Sea basin, offshore southwest Norway. *Norsk Geol. Tidskrift* 75, 105-119.

Gabrielsen, R. H., & Ramberg, B. 1979: Fracture patterns in Norway from LandSAT imagery:results and potential use. *Proc. Norwegian Sea Symp.*, Tromsø, Norwegian Petroleum Society, NSS/23, 1-28.

Gabrielsen, R. H., Odinsen, T, & Grunnaleite, I. 1999: Structuring of the Northern Viking Graben and the Møre Basin; the influence of basement structural grain and the particular role of the Møre Trøndelag Fault Complex. *Marine and Petroleum Geology* 16, 443-465.

Gallagher, K., Brown, R., & Johnson, C. 1998: Fission track analysis and its applications to geological problems. *Annual Review Earth Planetary Science* 26: 519-572.

Gee, D. G., Guezou, J. C., Roberts, D., & Wolff, F. C. 1985: The central-southern part of the Scandinavian Caledonides. *In* Gee, D. G. and Sturt, B. A. (eds.) *The Caledonian orogen – Scandinavia and related areas.* John Wiley and Sons, Chichester, 109-133.

Grønlie, A. & Roberts, D. 1990: Preliminary fission track ages of flourite mineralisation along fracture zones, inner Trondheimsfjord, central Norway. *Norsk Geologisk Tidsskrift*, 70.

Grønlie, A. & Roberts, D. 1989: Resurgent strike slip duplex development along the Hitra-Snåsa and Verran Faults, Møre-Trøndelag Fault Zone, Central Norway, Journal of Structural Geology, 11, 3, 295-305.

Grønlie, A. & Torsvik, T. 1989: On the origin and age of hydrothermal thorium enriched carbonate veins and breccias in the Møre Trøndelag Fault Zone, central Norway. *Norsk Geologisk Tidsskrift*, 69, 1-19.

Grønlie, A., Naeser, C. W., Naeser, N. D., Mitchell, J. G., Sturt, B. A., & Ineson, P. 1994: Fission track and K/Ar dating of tectonic activity in a transect across the MøreTrøndelag Fault Zone, Central Norway. *Norsk Geologisk Tidssrift* 74, 24-34.

Holtedahl, H. 1953: On the oblique uplift of some northern lands, *Norsk Geogr. Tidsskr.*, 14, 132-139.

Hobbs, W. H. 1911: Repeating patterns in the relief and structure of the land. *Geol. Soc. Am. Bull.* 22, pp. 123-176.

Hurich, C. A. & Kristoffersen, Y. 1988: Deep structure of the Caledonide orogen in southern Norway: new evidence from seismic reflection profiling. *Norges Geologiske UndersøkelseSpecial Publication*, 3, 96-101.

Hurich, C.A. & Roberts, D. 1997: A seismic reflection profile from Stjørdalen to Outer Fosen, Central Norway: a note on the principal results. (Extended abstract) *Norges Geologiske Undersøkelse Bulletin* 433, 18-19.

Kjerulf, T. 1879: Udsigt over det sydlige Norges geologi, *W. C. Fabritus*. Christiana (inc. atlas), pp. 262.

Laslett, G. M., Green, P. F., Duddy, I. R., & Gleadow, A. J. W. 1987: Thermal annealing of fission tracks in apatite, 2. A quantitative analysis. *Chem. Geol.* 65: 1-13.

Lundin, E. R. & Doré, A. G. 1997: A tectonic model for the Norwegian passive marginwith implications for the NE Atlantic: Early Cretaceous to breakup. *Journal of the Geological Society.* London. 154, 545-550.

Marrett, R., Ortega, O. & Kelsey, Celinda. 1999: Extent of power law scaling for natural fractures in rock. *Geology*, 27, 9, 799-802.

Milnes, A. G. & Koestler, A. G. 1985: Geological structure of Jotunheimen, southern Norway (Sognefjell-Valdres cross section. *In* Gee, D. & Sturt, B. A. (eds.): *The Caledonide Orogen - Scandinavia and Related areas,* 457-474. John Wiley & Sons, Chichester.

Mosar, J. (2000): Depth of the extensional faulting on the Mid-Norway Atlantic passive margin, Norges Geologiske Undersøkelse Bulletin. (In press.)

Olsen, A. E., Gabrielsen, R. H., & Redfield, T. 2000: Possible influence of offshore fracture zones in the Osen area, Trøndelag. *Geonytt*, Trondheim, 2000, 131.

Olesen, O., Gellein, J., Håbrekke, H., Kihle, O., Skilbrei, J. R. & Smethurst, M. A. 1997: Magnetic anomaly map, Norway and adjacent ocean areas. Scale 1:3 million. Norwegian Geological Survey.

Olesen, O. 1988: The Stuoragurra Fault: evidence of neotectonics in the Precambrian of Finnmark, northern Norway. *Norsk Geologisk Tidskrift* 68, 107-118.

Pascal, C., and Gabrielsen, R. H. (submitted): Numerical modeling of Cenozoic stress patterns in the mid Norwegian margin and the northern North Sea, *Tectonics.*

Ramberg, I, Gabrielsen, R. H., Larsen, B., & Solli, A. 1977: Analysis of fracture patterns in southern Norway. *Geol. en Mijnbouw* 56, 295-310.

Rindstad, B. I., & Grønlie, A. 1986: LandSAT TM data used in the mapping of large scale geological structures in coastal areas of Trøndelag, Central Norway. *In:* Proceedings of a Workshop on LandSAT Thematic Mapper applications. Frascati, Italy, December, 1987, 169-181.

Roberts, D. 1983: Devonian tectonic deformation in the Norwegian Caledonides and its regional perspectives. *Norges Geologiske Undersøkelse* 380, 85-96.

Rohrman, M. 1995: Thermal evolution of the Fennoscandian Region from Fission Track Thermochronolgy: an Integrated Approach, Vrije Universiteit Ph.D. Thesis, ISBN 90-9008814-8, 168 pp.

Rohrman, M., van der Beek, P., Andriessen, P. A. M., & Cloetingh, S. 1995: Meso-Cenozoic morphotectonic evolution of southern Norway: Neogene domal uplift inferred from apatite fission track thermochronology. *Tectonics* 14, 3, 704-718.

Seranne, M. 1992: Late Paleozoic kinematics of the MøreTrøndelag Fault Zone and adjacent areas, central Norway. *Norsk Geologisk Tidskrift.* 72, 141-158.

Stiberg, J. P. 1993: Apatite fission track analysis from the Western Gneiss Region, preliminary results: constraints to the Cenozoic uplift of the Norwegian passive margin (abstract). *Geonytt*, I, 46.

Stiberg, J. P., & Mørk, B. E. 1998: AFTA from the Western Gneiss Region: constraints on the Cretaceous - Cenozoic uplift of southwestern Norway. *TSGS*, Stavanger, 6-7.

Torske, T. 1972: Tertiary oblique uplift of western Fennoscandia; crustal warping in connection with rifting and breakup of the Laurasian continent, *Nor. Geol. Unders. Bull.*, 273, 43-48.

Torsvik, T. H., Sturt, B. A., Ramsay, D. M., Grønlie, A., Roberts, D., Smethhurst, M., Atakan, K., Bøe, R., & Walderhaug, H. J. 1989: Palaeomagnetic constraints on the early history of the MøreTrøndelag fault zone, central Norway. *In:* C. Kissel and C. Lai (eds.): *Paleomagnetic Rotations and Continental Deformation* 431-457, Kluwer Academic Publishers.

Torsvik, T. H., Sturt, B. A., Swensson, E., Andersen, T. B., & Dewey, J. F. 1992: Paleomagnetic dating of fault rocks: evidence for Permian and Mesozoic movements and brittle deformation along the extensional Dalsford fault, western Norway. *Geophys. J. Int.* 109. 565-580.

Torsvik, T. H., Mosar, J. & Eide, E. A., 2000: Cretaceous – Tertiary geodynamics – A north Atlantic exercise. *Geoph. J. International* (in review).

FIGURE CAPTIONS

Figure 1: Location map showing generalized geology after Andersen et al. (1999), Seranne (1992). Principal structures with a possible Mesozoic/Cenozoic history of movement include the Møre Trøndelag Fault Complex (MTFC) and the Hardangerfjord Shear Zone (HSZ). The study area is covered by three LandSAT TM5 images, shown in outline. Vikna Island and the Osen area of the Fosen Peninsula are located at the centers of the circles. Some of the known pre Tertiary faults and some of the principal bathymetric lineaments are shown offshore.

Figure 2a: Map of all lineaments in the MTFC region mapped at 1:100,000 scale from LandSAT TM5 images. Figure 2b: Frequency distribution diagram for all lineaments mapped. Lineaments greater than ~3km long and less than ~24km show the best correlation with a power law. Figure 2c: Map showing the subset of all lineaments greater then 3km and less than 2km in length.

Figure 3: Azimuth histogram showing azimuth distribution of all lineaments weighted by lineament length (red) and azimuth distribution of lineaments filtered to between 3km and 4km. Filtering resolves two small peaks at ~025 and ~090, but otherwise the azimuth distribution remains unaffected.

Figure 4: Two examples of lineament density grids. Top: output of 5km by 5km grid showing the density of all length filtered lineaments weighted by lineament length. Very high densities are noted in the NW portion of the study area. Bottom: output of 2.5km by 2.5km grid for the same data set. Discrete NESW trending structural zones are resolved.

Figure 5a: Interpretive map of the LandSAT TM5 images showing low correlation between well exposed areas (green) and poorly exposed areas (red) and lineament density. Figure 5b: Map showing the generalized geological contacts of the lithologically homogeneous Western Gneiss Region and the density of NW lineaments only. Significant variations of lineament density can be seen, indicationg lithology is not the only controlling factor.

Figure 6a: Geologic maps of Drag Fault, Grindvikna Fault, and Osen Fault. NNE trending Drag Fault (top left) contains many internally complex lenses of lithologically distinctive breccias. Many lenses are bounded by surfaces carrying steeply dipping slickenlines. Coarse, lightly mineralized protobreccias are clearly derived from the mylonitic gneiss host rock. Fragments of mylonite incorporated in the inner cataclasite lenses must have originated at much deeper levels, indicating significant net vertical offset. NNE trending Grindvikna Fault (middle) exposes multiple generations of breccia, calcite and sulfide mineralisation, steeply dipping slickenlines, and a 2 to 5 cm thick zone of unconsolidated fault gouge. N-S trending Osen Fault (bottom) exposes a narror but intensively deformed breccia with low angle slickenlines, calcite and sulfide mineralisation, and unconsolidated fault gouge.

Figure 6b: Top: LandSAT mosaic map showing the locations of Drag Fault and Grindvikna Fault and fracture lineaments of the surrounding region. The two faults are in left stepping relationship and form rhomboid patterns with strongly expressed, now drowned, NE trending lineaments parallel to the main trend of the MTFC. Bottom: LandSAT mosaic map showing the location of Osen Fault and other regional structures. Osen Fault clearly crosscuts the prominent NE trending Caledonian foliation and may also crosscut nearby NW trending fracture lineaments. A possible right stepping relationship between Osen Fault and other N trending lineaments can be discerned. Both images are rectified with true north at the top of the page.

Figure 7: Top: Aeromagnetic map of Norway (Olesen et al., 1997) showing several prominent NE trending lineaments. One magnetic lineament correlates very well with the Hitra Snasa strand of the MTFC, the boundary between our middle and outer block. Bottom: Wallis filtered Bouguer gravity anomaly map (Fichler et al., in press) showing diffuse but recognizable local anomalies in the area between the inner and middle blocks.

Figure 8a: Diagram showing three structural blocks identified by LandSAT TM5 analysis, regional geophysical data, and geological data.

Figure 8b: Showing two of 15 topographic and bathymetric profiles (solid blue lines) drawn across the MTFC (see Figure 8a for section locations). The solid red line shows the relative cross sectional area of each block. A down to the NW step function topography is evident.

Figure 8c: Weighted azimuth distribution of length filtered lineaments from each tectonic block. Weighting was achieved by multiplying azimuth by lineament length prior to creating a five degree band width histogram. Each histogram band was then divided by the total area of its tectonic block in order to normalize the histograms to one another. Densities of NESW and NWSE lineaments decrease from NW to SE. The densities of the NS and EW lineaments are unaffected by geography. The NWSE structures are the most geographically dependant, occurring dominantly in the outer block.

Figure 9a: Concordance diagram showing AFT data from Grønlie et al. (1994), Rohrman et al. (1995), and Stiberg (1993). Examination of error bars show the ages to be concordant at the 95% confidence level in three broad categories: 124-128Ma, 203-224Ma, and an older suite circa 260-320Ma (Stiberg and Mørk, 1998). The Jotunheim profeile of Rohrman et al. (1995) is reproduced to show the maximum plausible AFT ages of the inner block.

Figure 9b: Showing the distribution of AFT data cited in this study with respect to principal structures such as the MTFC, the Dalsfjord Fault, the HSZ, and the LGFS.

Figure 10: Tectonic model integrating the cited AFT data with regional geology compiled by Mosar et al. (in press). In the upper diagram the three tectonic blocks are shown at circa 300Ma, 200Ma, 100Ma, and the present. Today's zero elevation AFT age distribution is shown on the right. The starting point (circa 300Ma) is shown at left. Because track length histograms require slow rather than rapid cooling the AFT ages cannot be interpreted in terms of a discrete closure temperature. Rather, the ages represent a time when the annealing process was sharply reduced as the rock column cooled to lower temperatures near the upper part of the apatite Partial Annealing Zone (PAZ). The schematic block diagram shows one possible exhumation history for the Møre Trøndelag region. The lower diagram places the blocks into a lithospheric scale cross section incorporating onshore and offshore seismic data and geologic data (Mosar, in press). Known structures exist near the boundaries of the actual tectonic blocks (Figure 8a; cross section, above), showing the thermochronometric data fit independently derived tectonic and structural constraints.

Table 1: Table listing AFT literature data cited in this study. Tabulated elevations, AFT ages, track lengths, and errors are quoted from the original publications. Blanks exist where no data were listed. Samples locatare located in ED50 Zone 32 UTM coordinates. The quality of listed location data varies. Data published by Rohrman et al. (1995) are located to the nearest kilometer (see Rohrman, 1995). Data published by Grønlie et al. (1994) and Stiberg (1993) were not tabulated in the original publications. We relocated these samples using digitizing technology, a high quality digital topographic map, listed elevations, and the assumption that all samples were taken from roadside outcrops. The UTM coordinates for these are probably accurate to the nearest one to five kilometers. All ages were computed by the External Detector Method (see Gallagher et al., 1998). Additional AFT statistics will be found in the original publications.

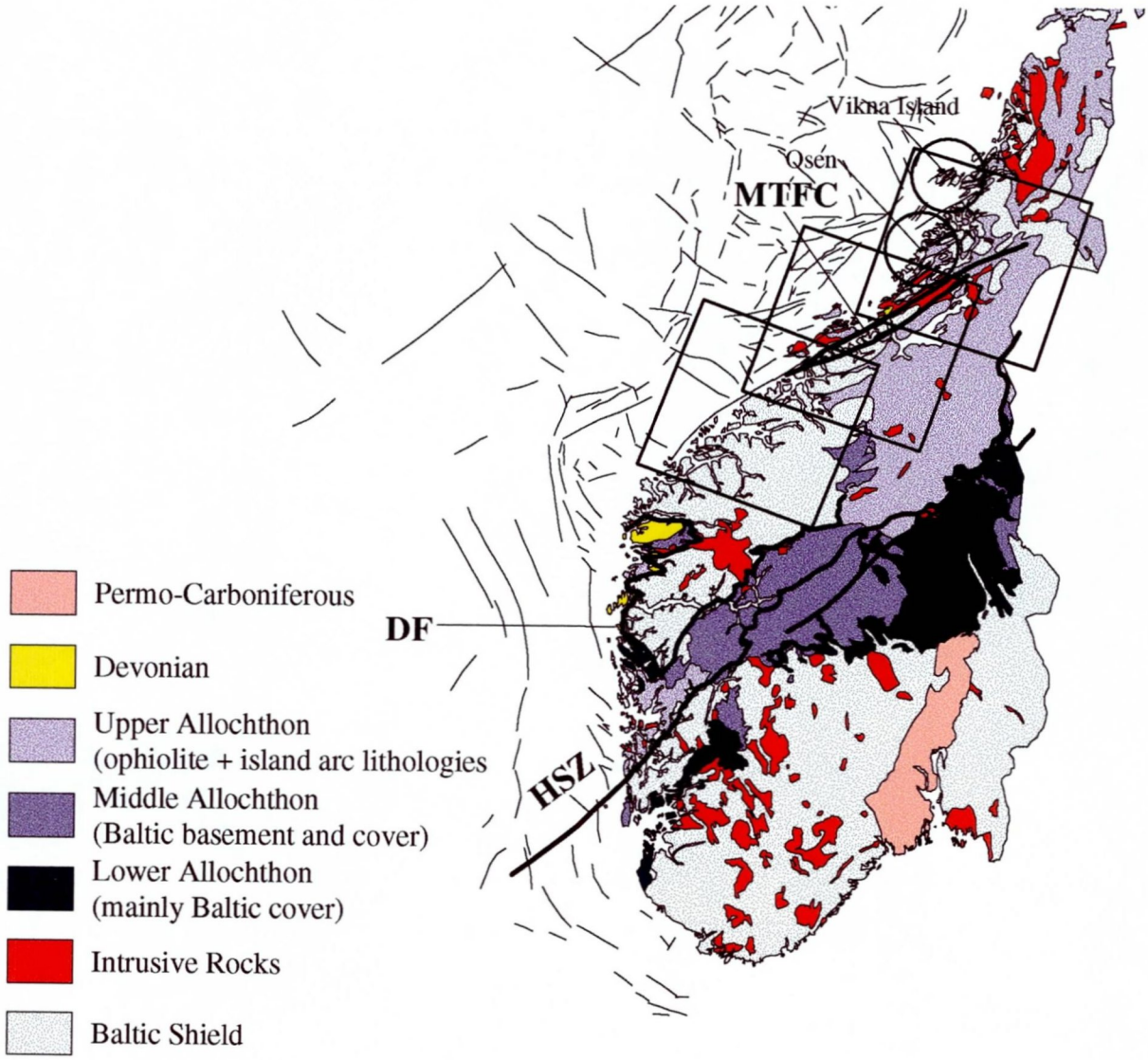
Vikna Island
Qsén
MTFC
DF
HSZ
Permo-Carboniferous
Devonian
Upper Allochthon
(ophiolite + island arc lithologies
Middle Allochthon
(Baltic basement and cover)
Lower Allochthon
(mainly Baltic cover)
Intrusive Rocks
Baltic Shield

Figure 1.

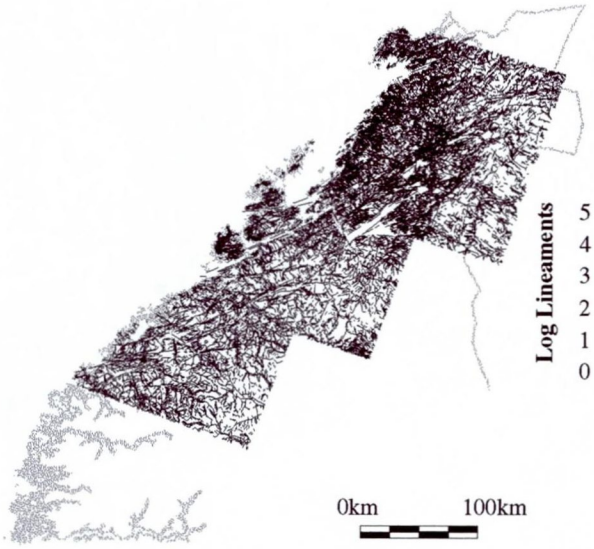

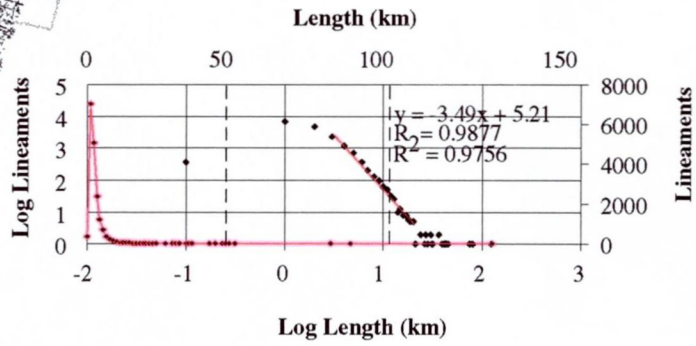

Figure 2b: Frequency diagram for all fracture lineaments. Lineaments greater than ~3km long and less than ~24km long show the correlation with a power law.

Figure 2a (above): Map of all 1:100,000 scale lineaments mapped from LandSAT TM5 images in the MTFC region.

Figure 2c (right): Map showing the subset of all lineaments greater than 3km and less than 24km in length.

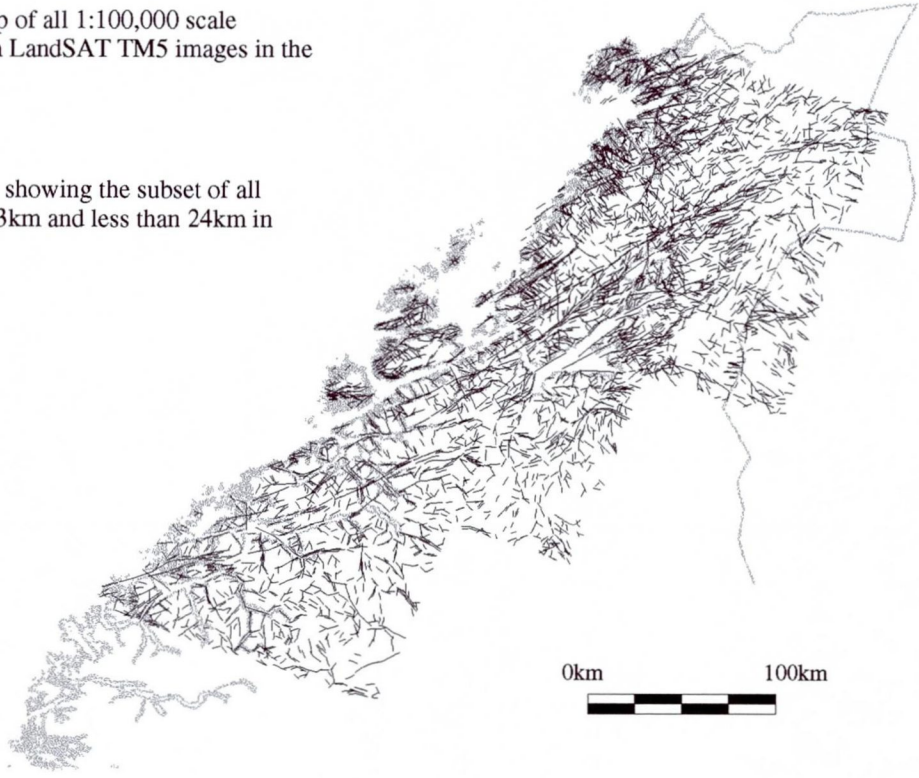

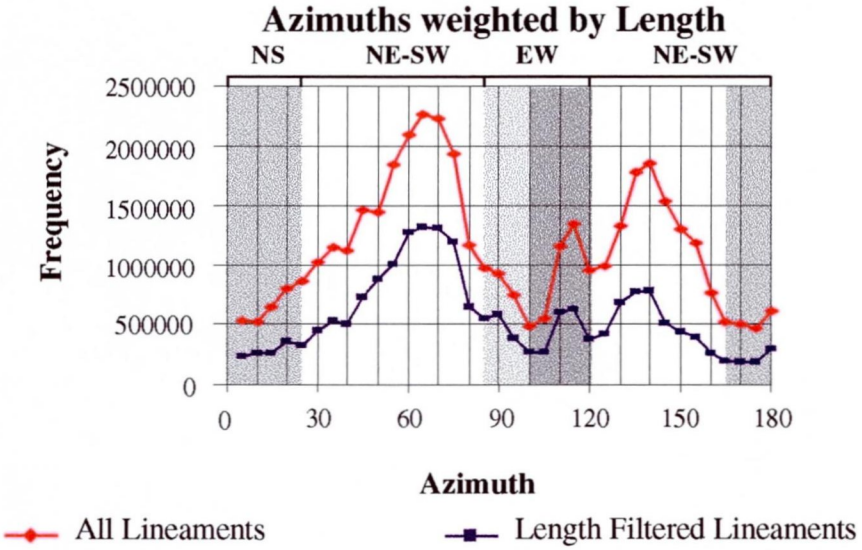

Figure 3

Histogram showing the azimuth distribution of all lineaments weighted by length (red) and lineaments greater than 3km and less than 24km in length (blue). Azimuths were weighted by lineament length prior to inclusion in the histogram.

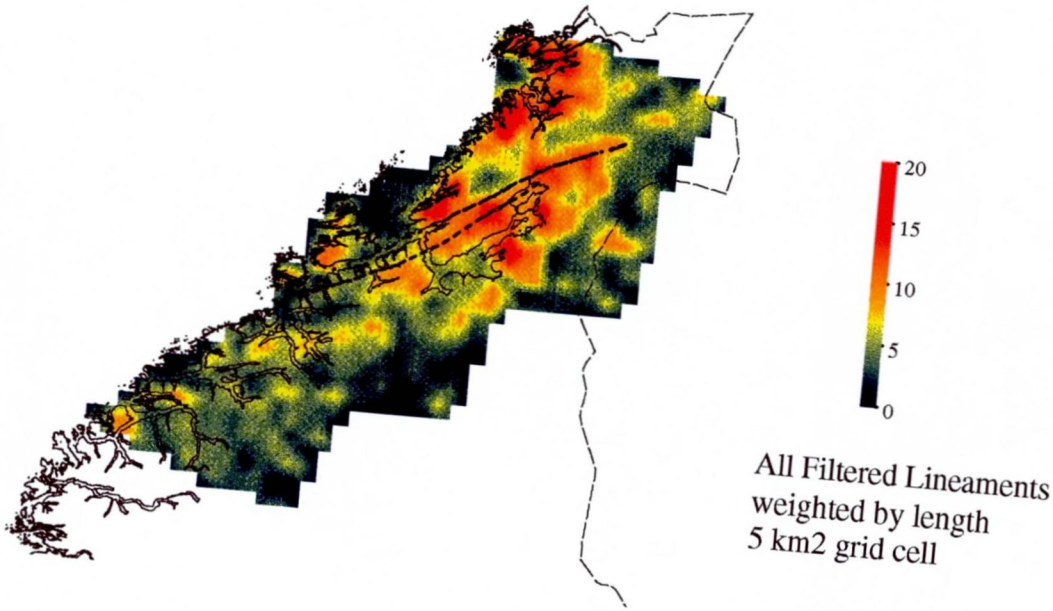
20
15
10
5
0
All Filtered Lineaments
weighted by length
5 km2 grid cell

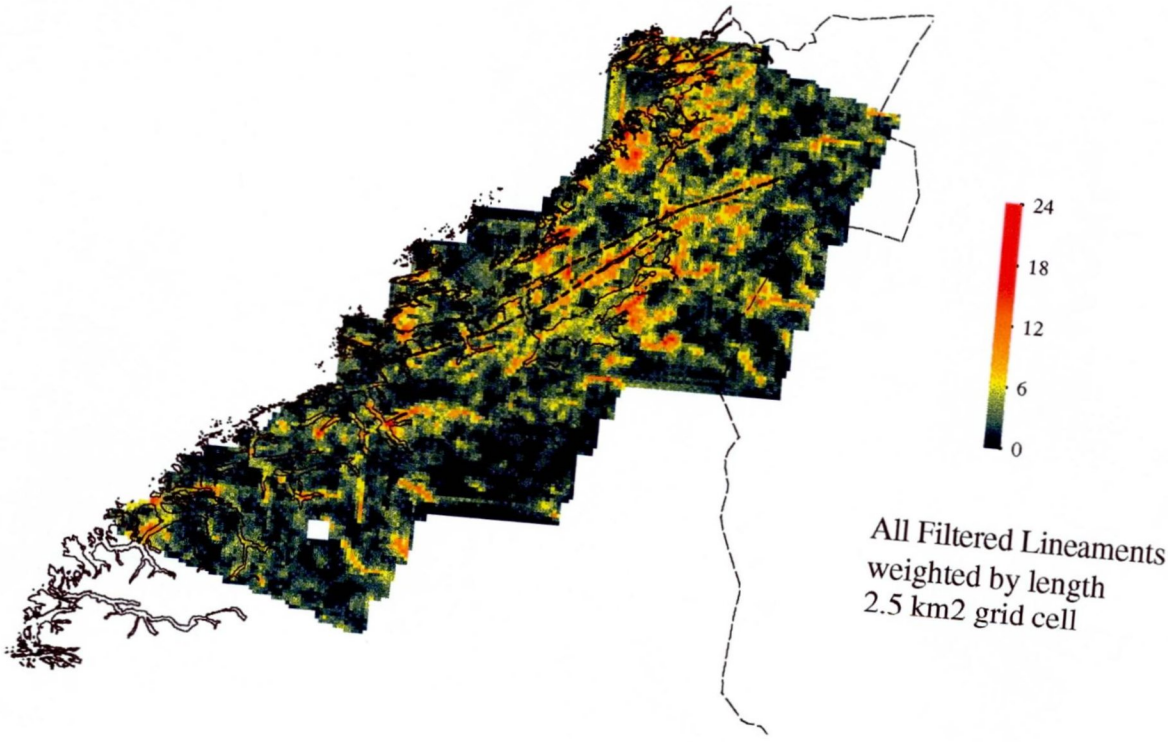
24
18
12
6
0
All Filtered Lineaments
weighted by length
2.5 km2 grid cell

Figure 4.

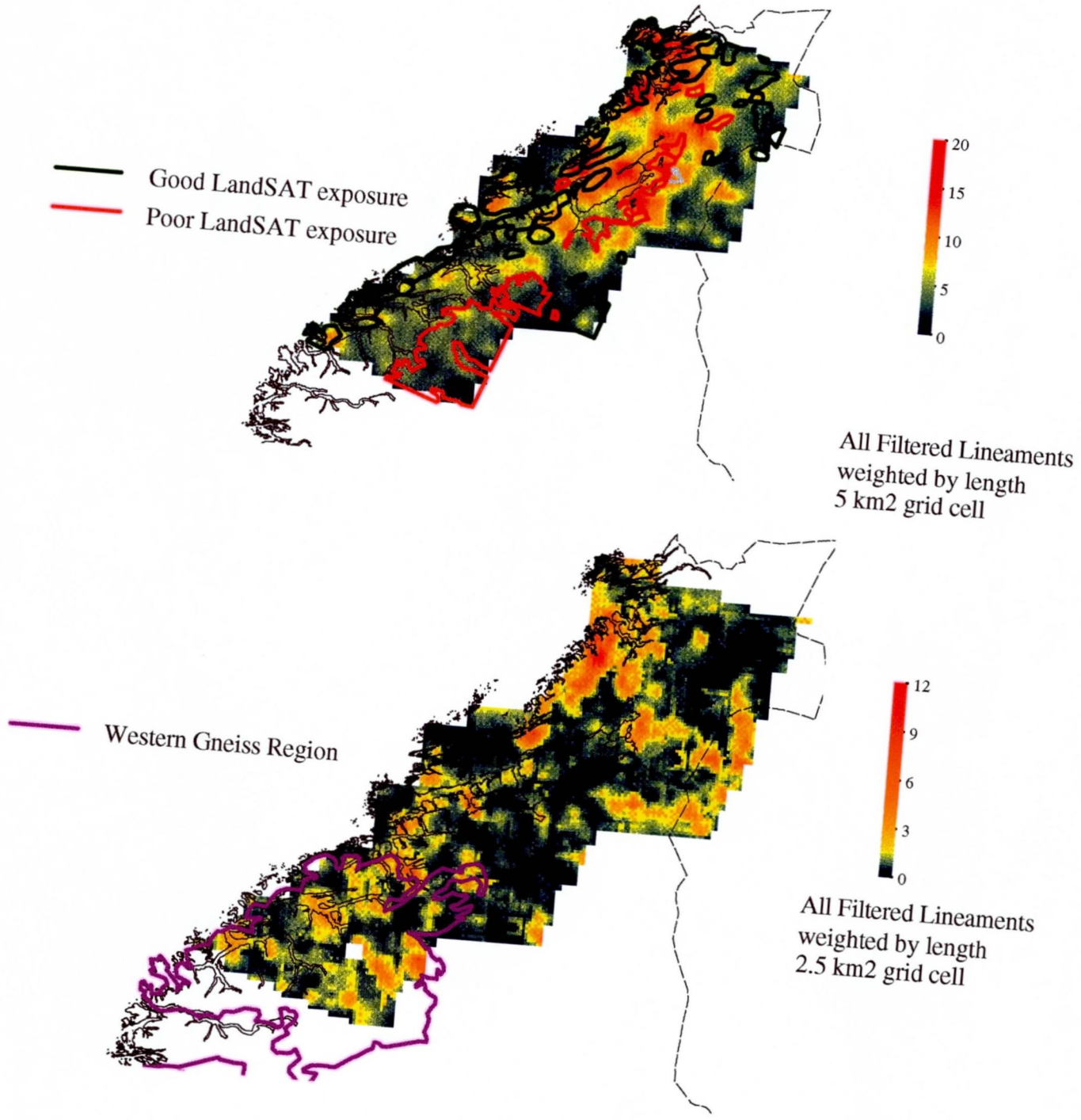
Good LandSAT exposure
Poor LandSAT exposure
20
15
10
5
0
All Filtered Lineaments
weighted by length
5 km2 grid cell
Western Gneiss Region
12
9
6
3
0
All Filtered Lineaments
weighted by length
2.5 km2 grid cell

Figure 5

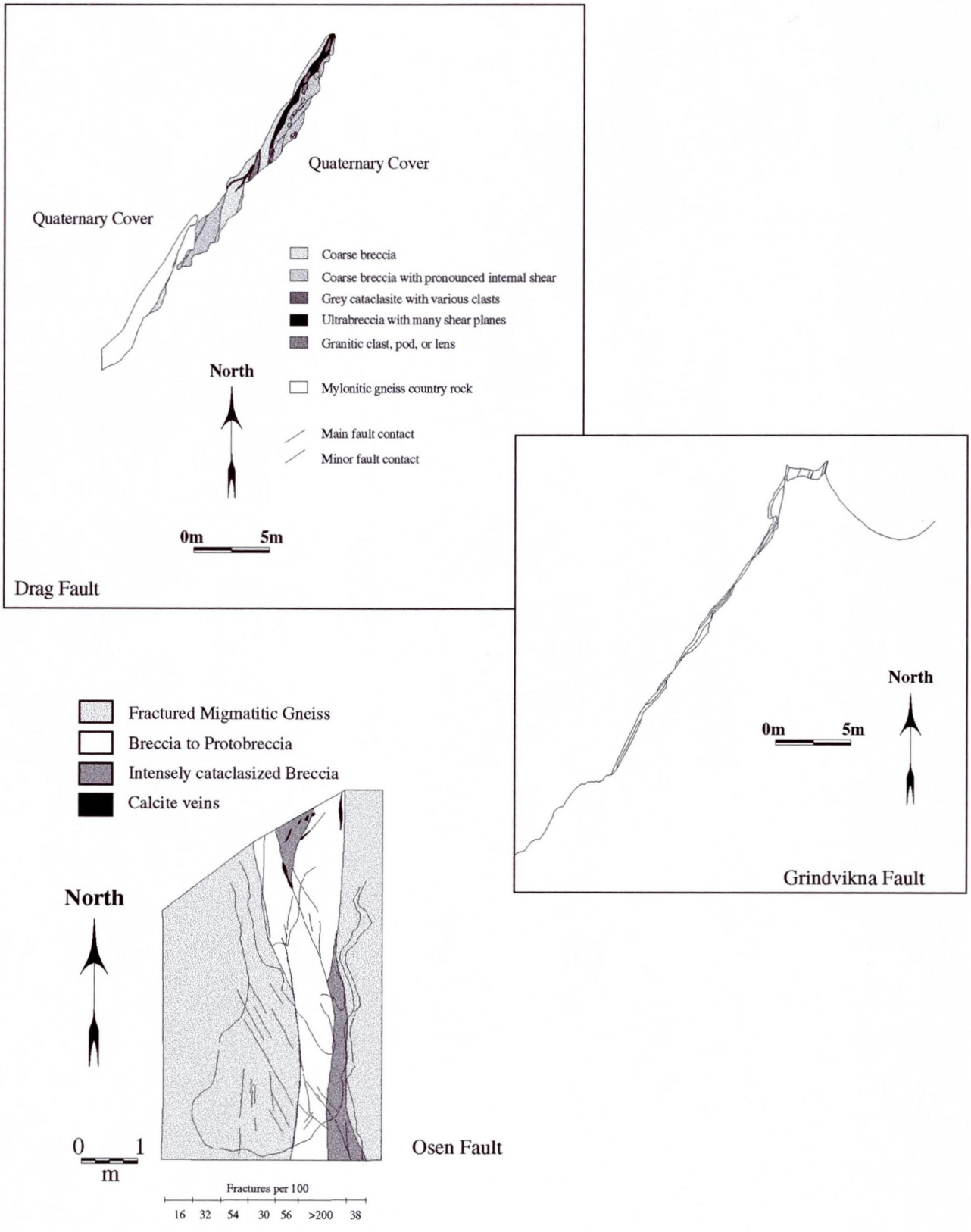
Quaternary Cover
Quaternary Cover
Coarse breccia
Coarse breccia with pronounced internal shear
Grey cataclasite with various clasts
Ultrabreccia with many shear planes
Granitic clast, pod, or lens
Mylonitic gneiss country rock
Main fault contact
Minor fault contact
North
0m
5m
Drag Fault
North
0m
5m
Grindvikna Fault
Fractured Migmatitic Gneiss
Breccia to Protobreccia
Intensely cataclasized Breccia
Calcite veins
North
0
1
m
Fractures per 100
16 32 54 30 56 >200 38
Osen Fault

Figure 6a

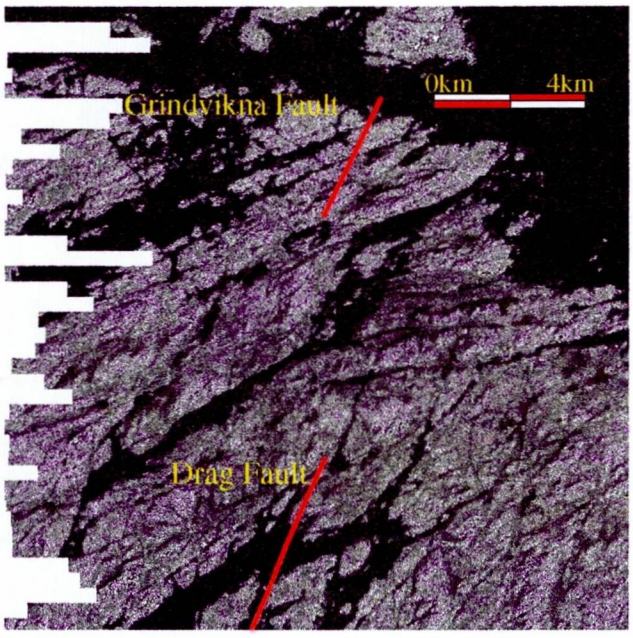

LandSAT mosaic mapshowing the locations of Drag Fault and Grindvikna Fault in regional context (left). The two faults are left stepping with respect to each other and form rhomboid shapes with prominent NESW lineaments parallel to the MTFC.

Images rectified to True Northat to of page.

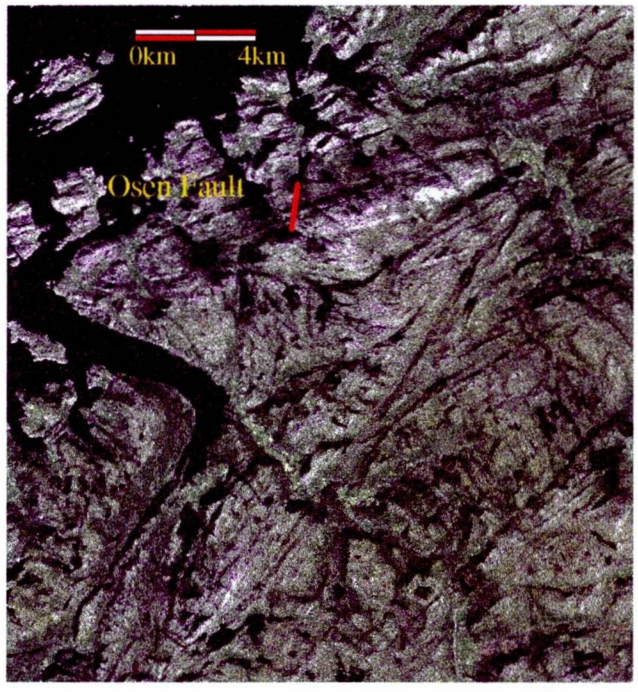

LandSAT mosaic map of Osen Fault (red) and other regional structures. Osen Fault clearly crosscuts the prominent NE trending Caledonian foliation and probably crosscuts nearby NW trending lineaments. A possible right stepping relationship between Osen Fault and other N trending lineaments can be discerned.

Figure 6b

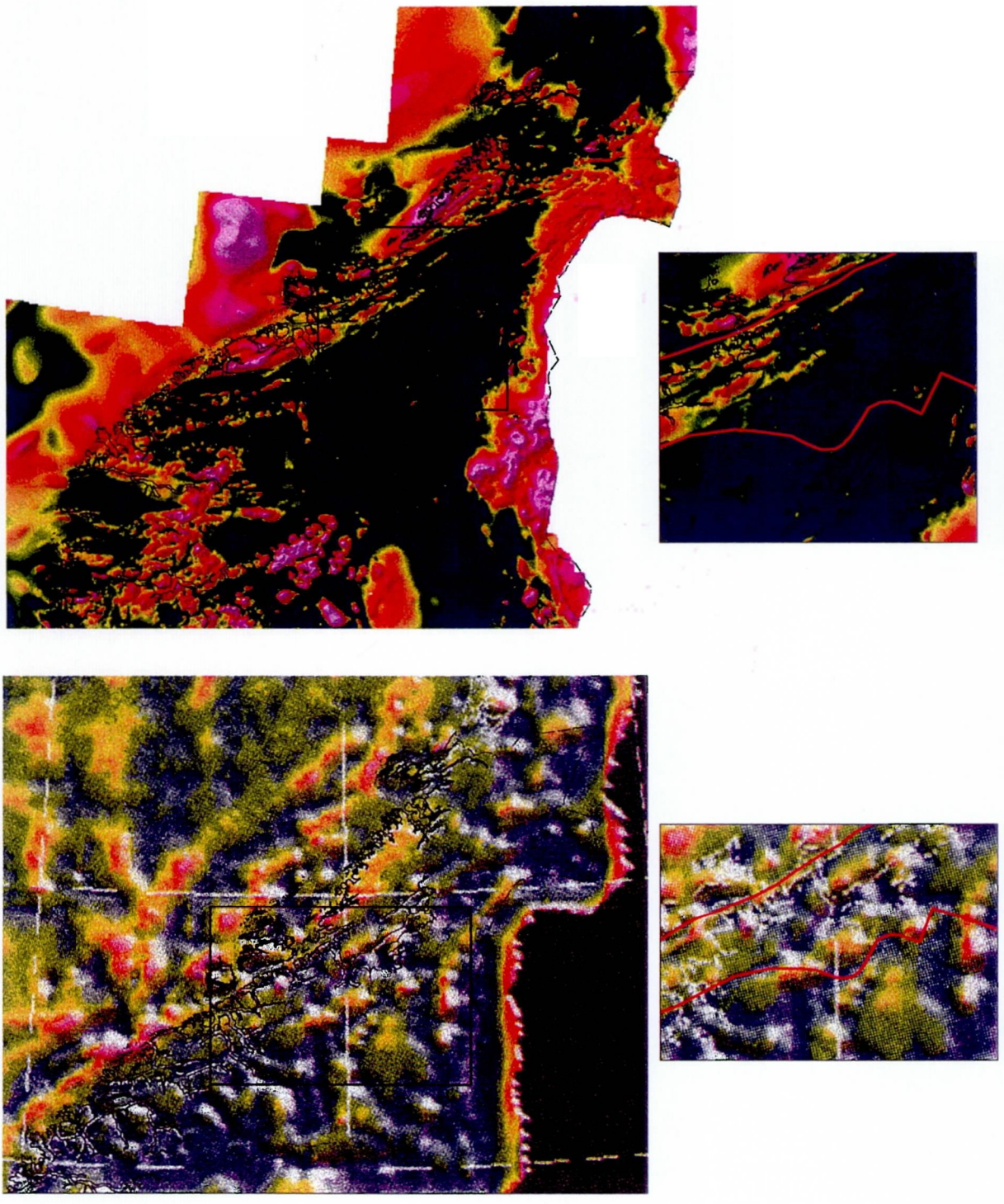

Figure 7

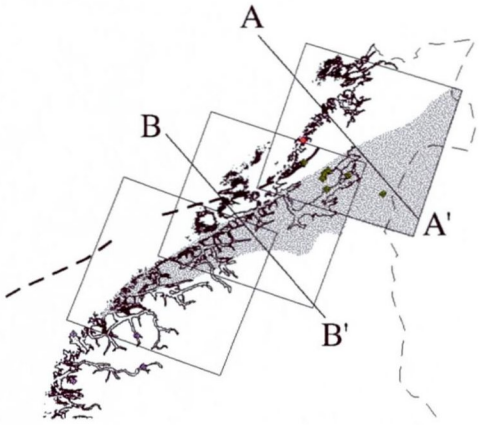

Figure 8a (above): Diagramshowing three structural blocks identified by LandSAT TM analysis, regional magnetic and gravity data, and geological data.

Figure 8b (right): Showing two of 15 topographi and /bathymetric profiles (solid blue line) drawn perpendicular to the MTFC. The solid red line shows the relative area of each block. A down-to-the-NW step topography is immediately apparent.

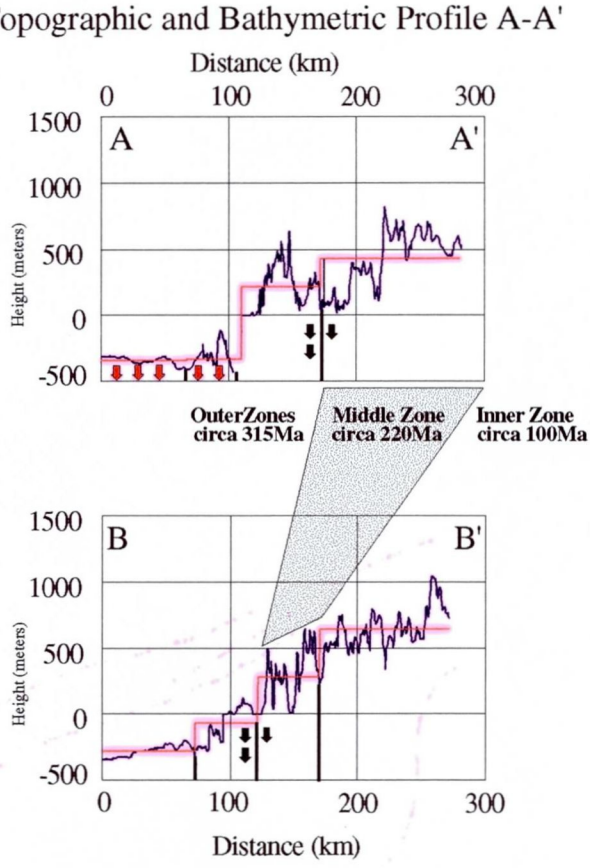

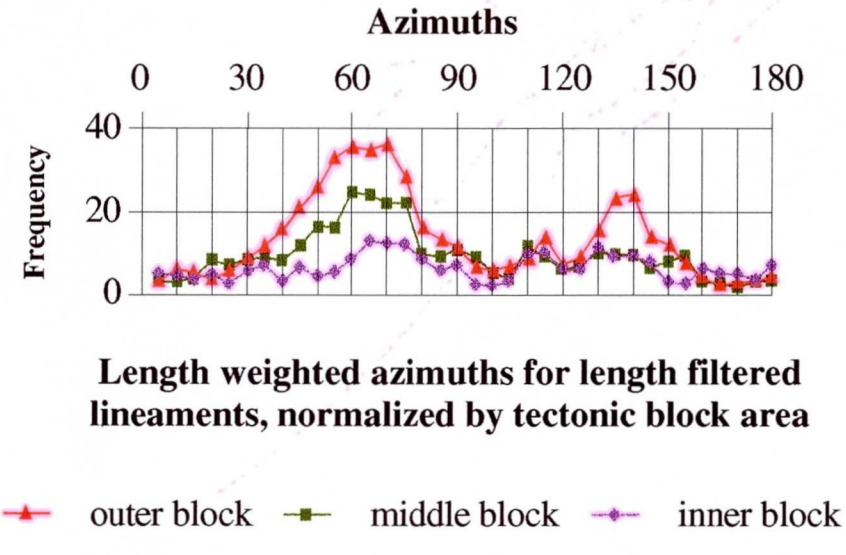

Figure 8c (left): Weighted azimuth distribution of length filtered lineaments (right) from the three tectonic blocks. Weighting was achieved by multiplying azimuth by lineament length prior to the creation of a 5 degree band histogram. Each histogram band was then divided by the total area of the appropriate tectonic block in order to normalize the Riemann sums of the histograms to one another. Densities of the NESW and NWSE lineaments decrease from NW to SE. The densities of the NS and EW lineaments are unaffected by geography. The NWSE structures are the most geographically dependant, occurring dominantly in the outer block.

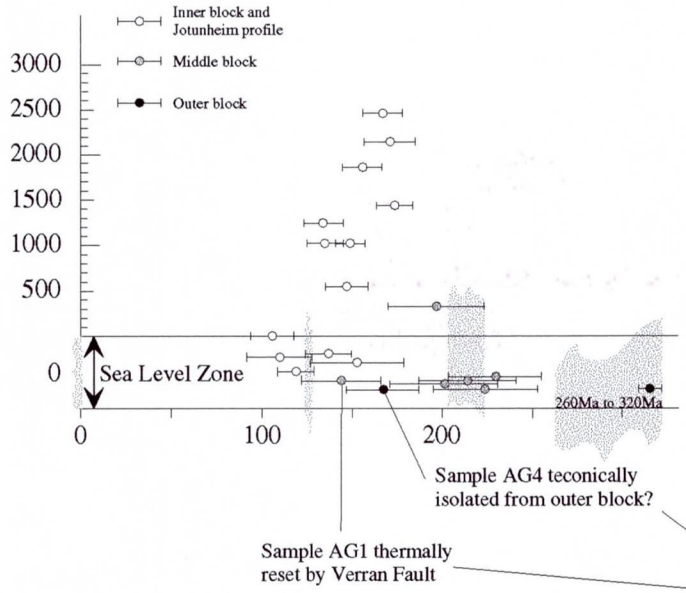

Figure 9a (left): ShowingAFT data from Grønlie et al. (1994), Rohrman et al. (1995) and Stiberg (1993). Examination of error bars show the ages to be concordant in three broad categories: 124-128Ma, 203-224Ma, and an older suite circa 260-320M (Stiberg and Mørk, 1998). The Jotunheim vertical profile of Rohrman et al. (1995) is reproduced to show the maximum plausible AFT ages of the inner block.

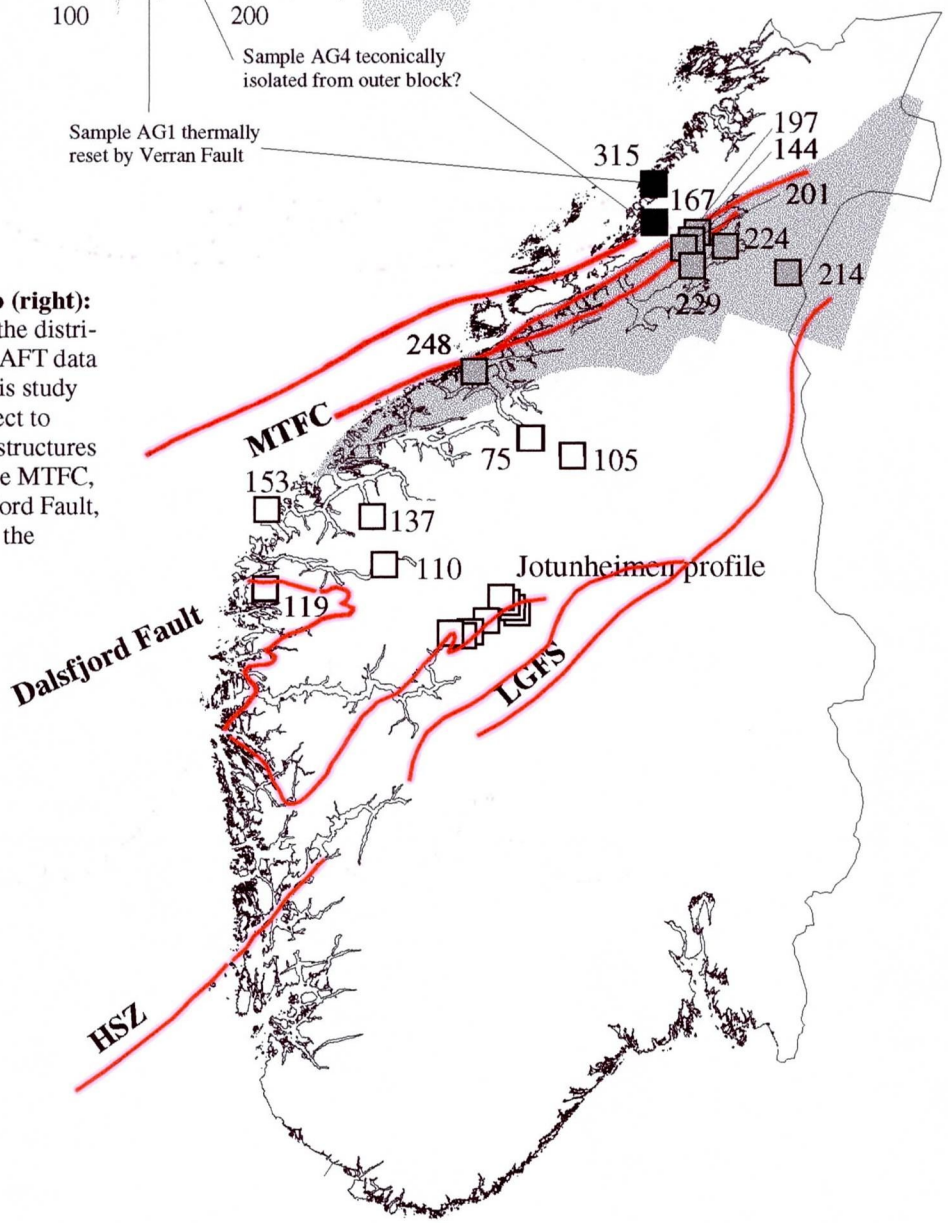

Figure 9b (right): Showing the distribution of AFT data used in this study with respect to principal structures such as the MTFC, the Dalsfjord Fault, HSZ, and the LGFS.

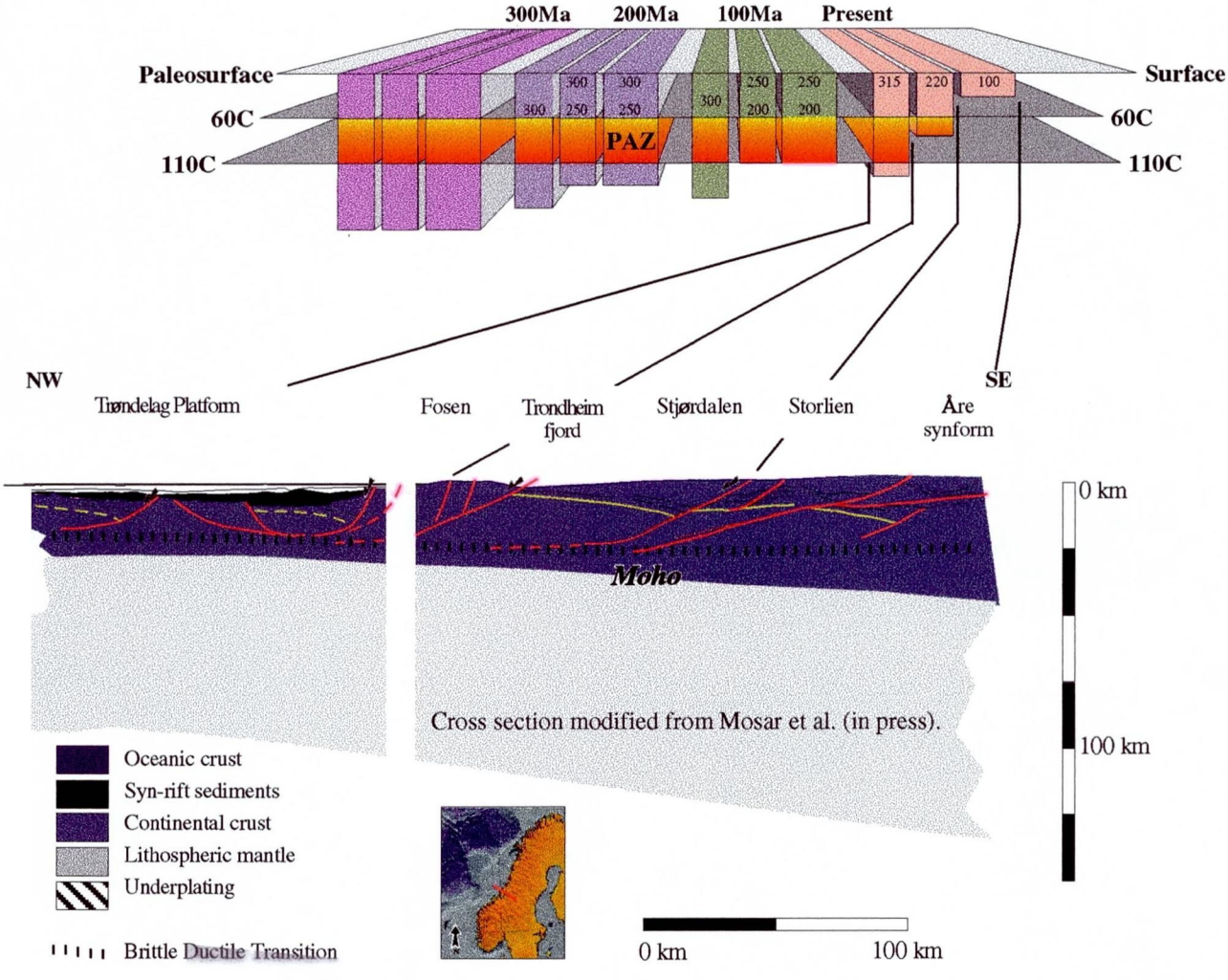

Figure 10.

Tectonic model integrating regional apatite fission track (AFT) data by Rorhman et al. (1985), Grønlie et al. (1994) and Stiberg (1993) with regional geology compiled by Mosar et al. (in press). In the upper diagram three tectonic blocks are shown at circa 300Ma, 200Ma, 100Ma, and the present. Today's zero elevation AFT age distribution is shown on the right (tan color). The starting point at circa 300Ma is shown on the left (purple). Because track length histograms show cooling was slow rather than rapid, the AFT ages cannot be interpreted in terms of a discrete closure temperature: the ages represent the time when the annealing process was sharply reduced as the rock column cooled to lower temperatures near the upper part of the apatite Partial Annealing Zone (PAZ, shown in flaming red). The schematic model depicts one possible exhumation history for the three blocks, requiring exhumation and relative down-to-the-NW gravity faulting. Although the model depicts only vertical movement, strike slip offset cannot be ruled out. The lower diagram places the tectonic blocks into a lithospheric scale cross section incorporating seismic data and geologic data. Known structures exist near the boundaries of the tectonic blocks, showing the thermochronometric data fit independently derived tectonic and structural constraints.

Table 1.

Sample	Elev(m)	Age	Error	Length	Error	Sdev	UTM East	UTM West	Author
FT2	50	224	29	NA			608000	7078000	Grønlie et al., 1994
FT5	100	229	26	13,19	0,18	1,43	585000	7064000	Grønlie et al., 1994
AG1	50	144	22	13,17	0,30	1,46	583000	7081000	Grønlie et al., 1994
AG2	460	197	27	13,73	0,17	1,20	586000	7085000	Grønlie et al., 1994
AG3	50	201	30	13,64	0,18	1,19	581000	7077000	Grønlie et al., 1994
AG4	50	167	20	13,95	0,13	1,30	560000	7093000	Grønlie et al., 1994
AG5	500	214	27	13,62	0,14	1,42	648000	7059000	Grønlie et al., 1994
93-3	0	119	10	12,50	0,20	1,50	302000	6849000	Rohrman et al., 1995
93-4	100	153	26				302000	6902000	Rohrman et al., 1995
93-5	0	137	13	12,00	0,30	0,90	372000	6900000	Rohrman et al., 1995
93-6	20	110	18				379000	6865000	Rohrman et al., 1995
Jot1	2465	167	11	13,50	0,10	1,20	464000	6834000	Rohrman et al., 1995
Jot3	2150	171	14	13,20	0,10	1,30	465000	6834000	Rohrman et al., 1995
Jot5	1855	156	11	13,40	0,10	1,20	467000	6833000	Rohrman et al., 1995
Jot9	1240	134	11				468000	6833000	Rohrman et al., 1995
Jot11	1430	175	10	12,60	0,10	1,20	447000	6827000	Rohrman et al., 1995
Jot12	1010	135	10	12,50	0,10	1,40	437000	6820000	Rohrman et al., 1995
Jot12	1010	149	8				437000	6820000	Rohrman et al., 1995
Jot14	560	147	12				434000	6819000	Rohrman et al., 1995
Jot17	0	106	12	11,60	0,20	2,00	425000	6819000	Rohrman et al., 1995
Roan	0	315					559000	7119000	Stiberg, 1993
Kristiansund	0	248					437000	6994000	Stiberg, 1993
Sundalsøra	0	75					476800	6949100	Stiberg, 1993
Aursjøen	850	105					505000	6937000	Stiberg, 1993